

Butadiene Insertion and Constitutional Units in Ethene Copolymerizations by C_2 -Symmetric Metallocenes

Pasquale Longo,* Mariagrazia Napoli, Stefania Pragliola, Chiara Costabile, Giuseppe Milano, and Gaetano Guerra

Dipartimento di Chimica, Università di Salerno, I-84081 Baronissi (SA), Italy

Received June 18, 2003; Revised Manuscript Received September 22, 2003

ABSTRACT: Copolymerizations of ethylene with 1,3-butadiene in the presence of catalytic systems based on some C_2 -symmetric zirconocenes (rac -[CH₂(3-R-1-indenyl)₂]ZrCl₂ where R = -C(CH₃)₃ (**1**), -CH(CH₃)₂ (**2**), -CH₂CH₃ (**3**), -CH₃ (**4**), and -H (**5**)) are compared. The chemical nature and the relative amount of constitutional comonomer units from butadiene are strongly affected by the bulkiness of the substituent in positions 3 and 3'. DFT calculations indicate that the observed dependence of constitutional units from butadiene on the bulkiness of the alkyl ligand substituent can be easily rationalized by the occurrence of an unusual insertion mechanism for butadiene. This mechanism, involving butadiene η^2 primary coordination followed by its primary vinyl insertion, becomes largely predominant for catalytic systems based on the zirconocenes (**1**–**4**), which present R \geq CH₃. This kind of butadiene insertion mechanism is also able to account for the high stereoregularity which is observed for adjacent methylene-1,2-cyclopropane units.

Introduction

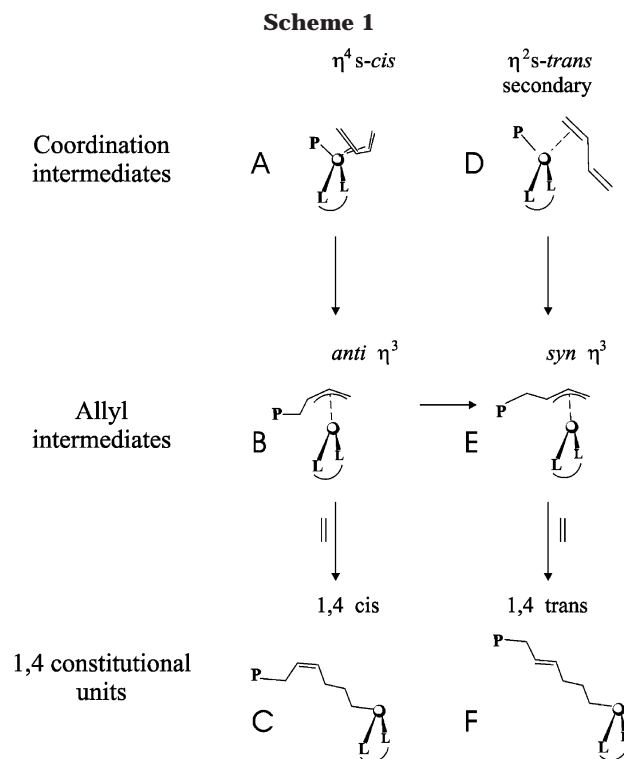
It is well-known that, by copolymerization of 1,3-butadiene with ethene, by suitable metallocene or constrained geometry catalysts,^{1–3} together with the usual 1,4- and/or 1,2-butadiene constitutional units, methylene-1,2-cyclopentane units can be obtained.

Recently we have shown that copolymerization of 1,3-butadiene with ethene, catalyzed by the C_2 -symmetric metallocene rac -[CH₂(3-*tert*-butyl-1-indenyl)₂]ZrCl₂ (**1**), discovered by Resconi and co-workers,⁴ which presents a large gap aperture associated with large substituents, generally leads to ethene copolymers only containing unprecedented methylene-1,2-cyclopropane units together with methylene-1,2-cyclopentane units, both with high *trans* selectivity.⁵

More recently we have also shown that copolymerization of the same monomers with the same catalytic system, when conducted at high temperature and low ethene concentration, can lead to ethene copolymers only containing unprecedented 1,1 and 1,3 constitutional units from 1,3-butadiene, both presenting only the *E* configuration of the double bond.⁶

It is generally accepted that the formation of 1,4- and 1,2-butadiene constitutional units would be obtained by reactions involving a η^3 -allyl intermediate. This would be generally produced by the insertion into the growing polymer chain of an η^4 *s-cis* coordinated butadiene (A in Scheme 1).⁷ In particular, *cis*-1,4-butadiene units (C) would be achieved from the *anti*- η^3 -coordinated growing chain (B) kinetic product of the insertion of the η^4 *s-cis* coordinated butadiene (A), while *trans*-1,4-butadiene units (F) would be generally achieved by isomerization reactions from the *anti*- η^3 -coordinated growing chain (B), toward the thermodynamically more stable *syn*- η^3 -coordinated growing chain (E).⁸

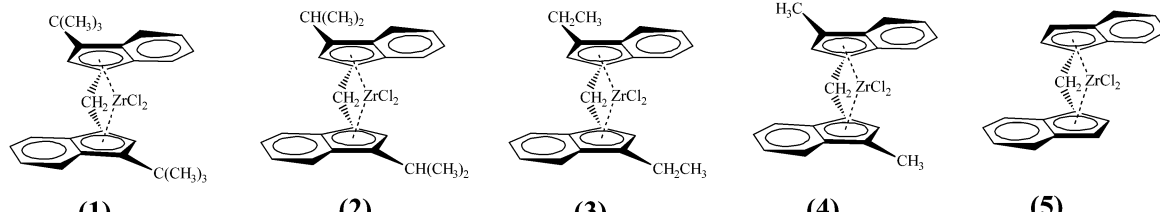
On the basis of experimental and modeling studies,^{5,6} the formation of 1,2-cyclopentane, 1,2-cyclopropane, and 1,1 and 1,3 constitutional units has been rationalized



by the reactions sketched in Scheme 2.⁶ According to this reaction scheme, all these new kinds of butadiene constitutional units would be obtained by rearrangements of a same intermediate (B in Scheme 2) which would be achieved by an unusual *primary vinyl insertion* of a η^2 -coordinated butadiene into a growing polymeric chain (σ -bonded to the metal) (A in Scheme 2).

It is worth recalling that metallocene based polymerization catalytic systems are generally highly regioselective in favor of primary (or 1,2) propene insertion.⁹ In particular, the regioselectivity of syndiospecific or aspecific systems is nearly complete,¹⁰ while substantial amounts of regioirregularities are obtained for isospe-

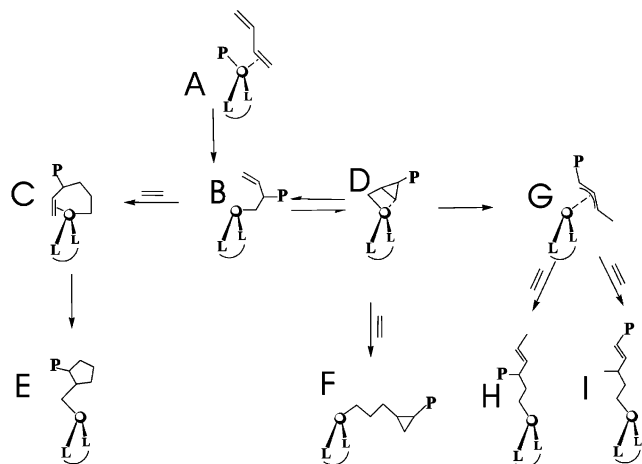
* Corresponding author. E-mail: plongo@unisa.it.

Table 1. Copolymerizations of Ethylene–1,3-Butadiene in the Presence of *rac*-[CH₂(3-R-1-indenyl)₂]ZrCl₂


Chemical structures of catalysts 1-5 are shown above the table. They are *rac*-[CH₂(3-R-1-indenyl)₂]ZrCl₂ where R = -C(CH₃)₃ (1), -CH(CH₃)₂ (2), -CH₂CH₃ (3), -CH₃ (4), and -H (5).

run ^a	catalyst	[B]	[E]/[B]	time (h)	yield (g)	<i>T</i> (°C)	<i>X</i> _B ^b	<i>f</i> _{BA} ^c	<i>f</i> _{BO} ^c	<i>f</i> _{B1,1} ^c	<i>f</i> _{B1,3} ^c	<i>f</i> _{B1,4} ^c	<i>T</i> _m ^d (°C)
1	1	0.52	0.31	16	3.5	20	0.03	0.64	0.36				112
2	2	0.51	0.32	5	1.5	20	0.06	0.11	0.71	0.08	0.10		81
3	3	0.51	0.32	17	2.7	20	0.06		>0.99				117
4	4	0.52	0.31	16	2.4	20	0.08		>0.99				118
5	5	0.50	0.32	16	1.1	20	0.15		0.39			0.61	119
6	1	0.51	0.21	1.5	2.0	50	0.04	0.14	0.04	0.61	0.20		114
7	2	0.52	0.20	1.8	1.5	50	0.06	0.03	0.26	0.42	0.28	0.01	83
8	3	0.51	0.21	1.5	1.5	50	0.08	0.02	0.17	0.50	0.28	0.03	80
9	4	0.52	0.20	3.0	3.1	50	0.05	0.03	0.89	0.02	0.02	0.03	112
10	5	0.53	0.20	1.5	1.6	50	0.06		0.53			0.47	118

^a Polymerizations were carried out by using 1×10^{-5} mol of zirconocene and 1×10^{-2} mol of MAO (based on Al). ^b Molar fraction of butadiene units in the copolymer chains. ^c Fraction of butadiene leading to cyclopropane ring units (*f*_{BA}), cyclopentane ring units (*f*_{BO}), 1,1 units (*f*_{B1,1}), 1,3 units (*f*_{B1,3}), and 1,4 units (*f*_{B1,4}). ^d Melting temperature.

Scheme 2

cific catalytic systems based on zirconocenes and hafnocenes.¹¹ This complete regioselectivity has been rationalized by a mechanism involving the rotation of the coordinated monomer from the orientation suitable for secondary insertion toward that one suitable for primary insertion, which would not be available for the wrong enantioface coordinated to isospecific catalysts.^{10b}

A different mechanism of regioselectivity, which can be highly effective also for isospecific zirconocenes and hafnocenes, involves the inhibition of secondary monomer coordination, by nonbonded interactions with suitable substituents of the π -ligand, mainly in positions 3 and 3' of bridged *C*₂-symmetric bis(indenyl) ligands.^{4,12} Recent polymerization studies have shown that only this latter regioselectivity, due to π -ligand substitution, is retained for other hydrocarbon monomers, forcing them to unusual reaction paths also leading to new polymeric structures.^{5,6,13} In particular, beside the above cited unprecedented methylene-1,2-cyclopropane, 1,1 and 1,3 constitutional units from butadiene, the catalytic system 1/MAO promotes an unusual primary insertion, as

well as the blocky copolymerization of ethylene and styrene.¹⁴

In the present paper, the copolymerization reactions of ethylene with 1,3-butadiene in the presence of catalytic systems based on some *rac*-[CH₂(3-R-1-indenyl)₂]ZrCl₂ (where R = -C(CH₃)₃ (1), -CH(CH₃)₂ (2), -CH₂CH₃ (3), -CH₃ (4), and -H (5)) are compared. The aim is to establish the influence of the bulkiness of the substituent in positions 3 and 3' on the nature of the butadiene constitutional comonomer units.

In the attempt to rationalize the influence of metallocene substituents on the nature of the butadiene constitutional units, DFT calculations are presented for metallocenes 1 and 5 relative to the above cited different kinds of butadiene coordination and insertion: (i) η^2 primary coordination of butadiene leading through a primary vinyl insertion to a σ -coordinated growing chain (step A \rightarrow B, in Scheme 2); (ii) η^4 -s-cis coordination of butadiene leading to a anti- η^3 -coordinated growing chain (step A \rightarrow B, in Scheme 1), which after isomerization would lead to a syn- η^3 -coordinated growing chain (E in Scheme 1).

Because of the bulkiness of the considered metallocenes, also an additional possibility for butadiene coordination and insertion has been considered: (iii) η^2 s-trans secondary coordination of butadiene (D in Scheme 1) directly leading to a syn- η^3 -coordinated growing chain (E in Scheme 1).

Experimental Part

General Procedure. All the operations were performed under nitrogen atmosphere by using conventional Schlenk-line techniques. Toluene was refluxed over sodium diphenylketyl for 48 h and distilled before use. 1,3-Butadiene and ethylene were purchased from Società Ossigeno Napoli (SON) and used without further purification. Methylalumoxane was purchased by Witco and used as a solid after distillation of solvent. The catalysts, *rac*-(CH₂(3-R-1-indenyl)₂)ZrCl₂, were synthesized using the procedure reported in the literature for *rac*-(CH₂(3-*tert*-butyl-1-indenyl)₂)ZrCl₂.⁴

Ethylene-1,3-butadiene Copolymerizations. Runs 1–10. In a typical copolymerization procedure, a constant ethylene overpressure was applied to a solution of 1,3-butadiene (see

Table 2. Ethene–1,3-Butadiene Copolymerizations at High Ethene Pressure

run	catalyst	[B]	[E]/[B]	time (h)	yield (g)	T (°C)	X _B ^a	f _{BA} ^b	f _{BO} ^b	f _{B1,1} ^b	f _{B1,3} ^b	f _{B1,4} ^b
11	1	1.50	0.72	1	20.0	50	0.01	0.66	0.34			
12	2	0.68	1.27	1	28.3	50	0.04	0.05	0.28	0.38	0.29	
13	4	0.55	1.58	1	60.1	50	0.02		>0.99			

^a Molar fraction of butadiene units in the copolymer chains. ^b Fraction of butadiene leading to cyclopropane ring units (f_{BA}), cyclopentane ring units (f_{BO}), 1,1 units (f_{B1,1}), 1,3 units (f_{B1,3}), and 1,4 units (f_{B1,4}).

Table 1) and 0.3 g of MAO in 10 mL of dry toluene. After thermostating at reaction temperature, 1×10^{-5} mol of metallocene in 2 mL of dry toluene were added to the solution. All the copolymers were recovered by precipitation with ethanol/HCl and dried under reduced pressure at room temperature.

Runs 11–13. These runs were carried out in a 250 mL glass autoclave, thermostated at 50 °C, introducing into this 100 mL of toluene, MAO (10.0 mmol, 580 mg), the butadiene, and the catalyst (20.0 μmol), as reported in Table 2. The autoclave was fed with ethene (5 atm) and kept under magnetic stirring over the runs, and then it was vented and the polymerization mixture was recovered as usual.

Run 14. This run was performed at 20 °C, as runs 1–10, by utilizing 0.210 g (3.88 mmol) of butadiene. To the mixture was applied a constant ethylene overpressure of 6 cm of Vaseline (0.28 mmHg) during the run. The polymerization was stopped by injecting a few milliliters of ethanol and the polymer recovered as usual. The molar fraction of butadiene in the copolymer, evaluated by ¹³C NMR analysis, was 0.12. (f_{BA} = 0.41, f_{BO} = 0.08, f_{B1,1} = 0.24, f_{B1,3} = 0.12, f_{B1,2} = 0.15; where f_{BA}, f_{BO}, f_{B1,1}, f_{B1,3}, and f_{B1,2} are the fractions of butadiene leading to cyclopropane, cyclopentane, 1,1-, 1,3-, and 1,2-inserted units).

Polymer Analysis. NMR spectra were recorded on an AM 250 Bruker spectrometer operating at 62.89 MHz at 393 K. The samples were prepared by dissolving 40 mg of polymer in 0.5 mL of tetrachlorodideuteroethane. Hexamethyldisiloxane was used as internal chemical shift reference.

The resonances were assigned on the base of the data reported in the literature.⁶ The molar fractions of ethylene and butadiene (X_E and X_B) in the copolymers were calculated by the following equations:

$$X_E = E/(E + B); \quad X_B = B/(E + B)$$

$$E = \frac{1}{2}(\Sigma C_s - 2C_2 - 2C_{2'} - 2C_7 - 2C_{7'} - 2C_{15} - 2C_{20} - 2C_{21} - 2C_{25})$$

$$B = [1/2(C_2 + C_{2'} + C_7 + C_{7'} + C_{21}) + C_{15} + C_{20} + C_{25}]$$

$$f_{BA} = \frac{1}{2}(C_2 + C_{2'})/B$$

$$f_{BO} = \frac{1}{2}(C_7 + C_{7'})/B$$

$$f_{B1,1} = C_{15}/B$$

$$f_{B1,3} = C_{20}/B$$

$$f_{B1,4} = C_{21}/B$$

$$f_{B1,2} = C_{25}/B$$

where: E and B are the molar fractions of ethene and butadiene units in the polymer chain, respectively. f_{B1,4} is the fraction of butadiene leading to 1,4-inserted units. ΣC_s is the sum of the areas of the resonances of the all saturated carbons, the subscripts of carbon atoms are referred to those indicated in the inset model of Figure 1.

Computational Details. Stationary points on the potential energy surface were calculated with the Amsterdam density functional (ADF) program system,¹⁵ developed by Baerends et al.^{16,17} The electronic configuration of the molecular systems was described by a triple-basis set on zirconium for 4s, 4p, 4d, 5s, and 5p. Double-STO basis sets were used for carbon

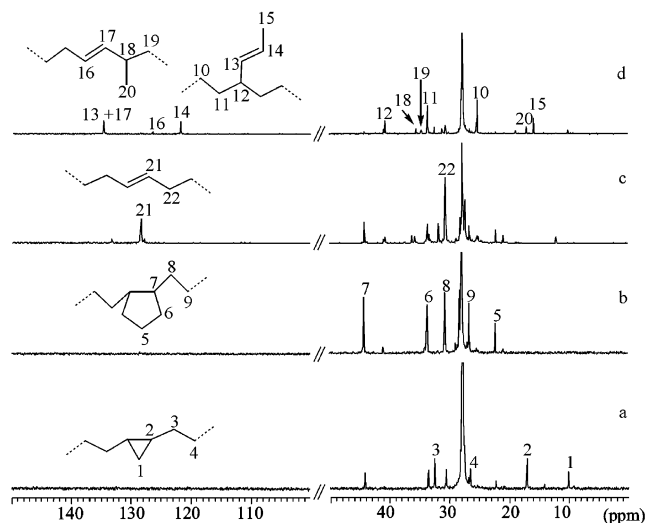


Figure 1. ¹³C NMR spectra of the samples obtained from the runs 1, 4, 5, and 6 of Table 1 (hexamethyldisiloxane scale). The inset models correspond to the main substructures.

(2s,2p) and hydrogen (1s), augmented with a single 4d, 3d, and 2p function, respectively. The inner shells on zirconium (including 3d) and carbon (1s) were treated within the frozen core approximation. Energetics and geometries were evaluated by using the local exchange-correlation potential by Vosko et al.,¹⁸ and augmented in a self-consistent manner with Becke's¹⁹ exchange-gradient correction and Perdew's^{20,21} correlation gradient correction. Geometry optimizations were terminated if the largest component of the Cartesian gradient was smaller than 0.002 au.

Results and Discussion

Polymerization Tests. In Table 1, the results of two set of copolymerization runs performed at 20 and 50 °C in the presence of catalytic precursors **1–5** are reported.

The runs were carried out utilizing for each temperature very similar reaction conditions, moreover since for catalyst **1** the formation of 1,3 and 1,1 constitutional units is suppressed by high ethene concentrations in the feed,⁶ low [ethene]/[butadiene] ratios have been used. The microstructure of the copolymers were fully determined by ¹³C NMR analysis, utilizing the attribution reported in the literature. The ¹³C NMR spectra of the samples obtained from the runs 1, 4, 5, and 6 of Table 1 are reported in Figure 1, parts a–d, respectively, together with the recognized substructures (inset models).

Observing the results of the runs at 20 °C (1–5), it is possible to note that increasing the bulkiness of the substituent in position 3 of the indenyl groups, the molar fraction of butadiene in the copolymers decreases, and there are substantial changes in the nature of the constitutional units from butadiene.

In agreement with previous polymerization tests,⁵ by metallocene **1**, all inserted butadiene molecules give rise to methylene-1,2-cyclopropane and methylene-1,2-cy-

cllopentane units in a ratio close to 2/1. The copolymer produced in the presence of **2** contains the inserted butadiene prevalingly as methylene-1,2-cyclopentane, but also as methylene-1,2-cyclopropane, 1,1 and 1,3 units, each in amount close to 10%. In the products obtained by metallocenes **3** and **4**, all the inserted butadiene generates methylene-1,2-cyclopentane units. The catalytic precursor **5**, in agreement with previous polymerization tests in similar conditions,⁵ produces a copolymer containing the highest molar fraction of butadiene, which is mainly inserted as 1,4-*trans* and as methylene-1,2-cyclopentane units.

The data of the runs performed at 50 °C and low ethene concentration (6–10 in Table 1), show that the molar fraction of butadiene for the obtained copolymers is poorly dependent on the catalytic system, and it is not simply related to the bulkiness of the substituent in position 3. In agreement with previous polymerization tests,⁶ at high temperature and low ethene concentration, catalyst **1** inserts butadiene mainly as 1,1 and 1,3 units. Similar behaviors are observed for copolymerization tests with catalysts **2** and **3**, which however also produce a substantial amount of 1,2-cyclopentane units together with minor amounts of 1,2-cyclopropane and *trans*-1,4 units. The increase of polymerization temperature from 20 up to 50 °C has only minor effects on the catalytic behavior of catalysts **4** and **5**. In particular, for catalyst **4**, the main insertion product remains 1,2-cyclopentane, and only a loss of selectivity is observed. As for catalyst **5**, the main inserted units remain *trans*-1,4- and 1,2-cyclopentane, but the ratio between the two units changes in favor of the cyclic one.

Selected polymerizations runs at 50 °C, which have been conducted at higher ethylene concentrations in the feed, are reported in Table 2.

These polymerization tests give high polymer yields (at least 20 g in 1 h) of copolymers with a fraction of butadiene units (X_B) in the range 0.01–0.04. A comparison between the polymerization tests of Table 1 (runs 6–10) and those of Table 2, shows that the influence of the ethene concentration in the feed on the relative amounts of the constitutional units from butadiene is markedly different for the different catalysts. In particular, a poor dependence is observed for catalyst **2** (cf. runs 12 and 7) while high ethylene concentration, for catalyst **1**, suppresses 1,1 and 1,3 units (cf. runs 11 and 6 and runs 5 and 6 of ref 6) and for catalyst **4**, suppresses 1,1 and 1,3 as well as methylene-1,2-cyclopropane units (cf. runs 13 and 9).

In the framework of the reactions of Scheme 2, the behavior of catalyst **2** could be rationalized by assuming that for all butadiene insertion routes the rate-determining step would be those involving ethene insertion (B → C, D → F, G → H, G → I) while the behavior of catalyst **4** could be rationalized by assuming that the rate-determining step would be B → C (involving ethene insertion) for cyclopentane formation and B → D (not involving ethene insertion) for the formation of the other units from butadiene.

Molecular Modeling of Butadiene Coordination and Insertion. Models corresponding to the mechanisms i–iii (i, which involves a η^2 primary coordination of butadiene and leads through a primary vinyl insertion to a σ -coordinated growing chain, ii, which involves a η^4 -s-cis coordination of butadiene and leads to a anti- η^3 -coordinated growing chain, and iii, which involves η^2 secondary coordination of butadiene directly leading to

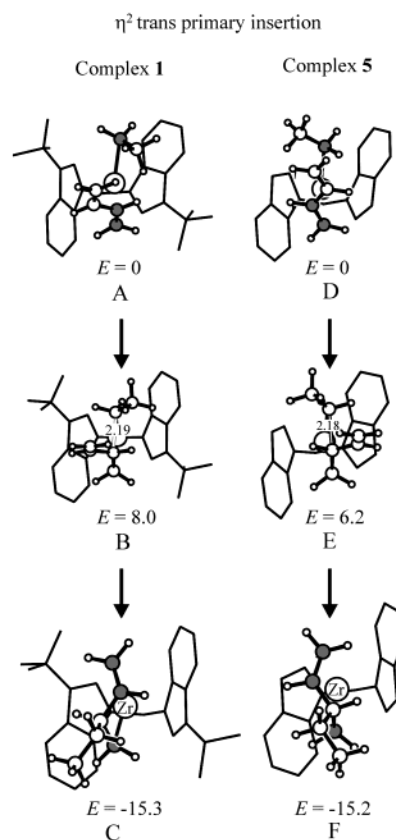


Figure 2. Models corresponding to mechanism i, which involves a η^2 primary coordination of butadiene and leads through a primary vinyl insertion to a σ -coordinated growing chain (step A → B of Scheme 2). Minimum energy monomer coordinated intermediates (A, D), transition states relative to the monomer insertion (B, E) and post-insertion intermediates (C, F), for catalysts **1** (A → B → C) and **5** (D → E → F). For the clarity of presentation, for all the intermediates, the carbon atoms of the monomer and of the growing chain, which are directly bonded to the metal, have been shown as gray spheres.

a syn- η^3 -coordinated growing chain) are shown in Figures 2–4, respectively, for both catalysts **1** (A → B → C) and **5** (D → E → F). For all mechanisms and for both catalysts, minimum energy monomer coordinated intermediates (A, D) and transition states relative to the monomer insertion (B, E) as well as post-insertion intermediates (C, F) have been reported. For the clarity of presentation, for all the intermediates, the carbon atoms of the monomer and of the growing chain, which are directly bonded to the metal, have been shown as gray spheres.

Minimum energy intermediates corresponding to the η^2 primary coordination of butadiene, shown in Figure 2, parts A and D, present a butadiene s-*trans* conformation and have been chosen as zero energy for catalysts **1** and **5**, respectively. The corresponding post-insertion minimum energy intermediates, which present a σ -coordinated growing chain (Figure 2, parts C and F), are stabilized by a backbiting coordination of the side chain double bond, which has been produced by the primary vinyl insertion of butadiene.

As for the classical mechanism which involves a η^4 cis coordination and insertion of butadiene (Figure 3), as well as for a possible mechanism which involves a η^2 secondary butadiene insertion (Figure 4), minimum energy intermediates and transition states present, for the unsubstituted catalyst **5**, energies similar to those calculated for the mechanism involving the η^2 primary

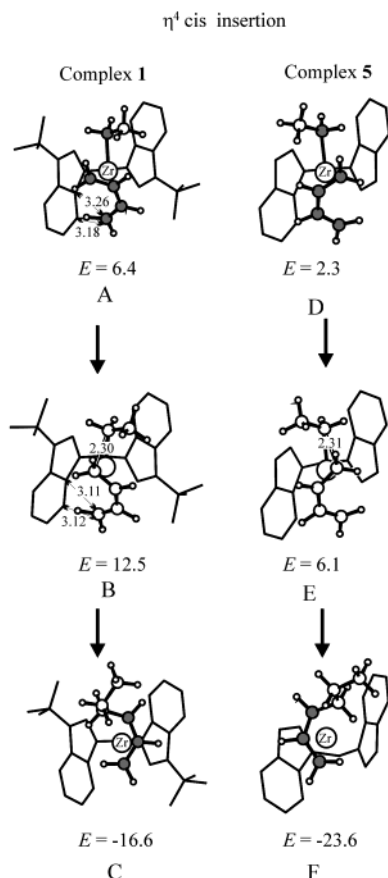


Figure 3. Models corresponding to mechanism ii, which involves a η^4 -s-cis coordination of butadiene and leads to a anti- η^3 -coordinated growing chain (step A \rightarrow B of Scheme 1). Minimum energy monomer coordinated intermediates (A, D), transition states relative to the monomer insertion (B, E) and post-insertion intermediates (C, F), for catalysts **1** (A \rightarrow B \rightarrow C) and **5** (D \rightarrow E \rightarrow F).

butadiene insertion (Figure 2) (cf. 2D, 3D, and 4D as well as 2E, 3E, and 4E). On the other hand, both mechanisms present definitely larger energies for the bulkier catalyst **1** (cf. 2A, 3A, and 4A as well as 2B, 3B, and 4B). In fact, as for catalyst **1**, both intermediates corresponding to η^4 -s-cis coordination of butadiene (Figure 3A) and η^2 s-trans secondary coordination of butadiene (Figure 4A) imply strong nonbonded interactions of the coordinated diene with the bulky cyclopentadienyl substituents (*tert*-butyl groups and six-membered rings). Similar repulsive nonbonded interactions are also present in the corresponding transition states (Figures 3B and 4B) leading to a anti- η^3 -coordinated growing chain (Figure 3C) and directly leading to a syn- η^3 -coordinated growing chain (Figure 4C), respectively.

It is also worth noting that the post insertion intermediates of mechanisms ii and iii, with η^3 -coordinated growing chains (Figures 3C,F and 4C,F), present energies generally much lower than post-insertion intermediates of mechanism i, which present a σ -coordinated backbiting growing chain (Figure 2C,F). As already described for a simplified model of catalyst **1**, in Figure 3 of ref 6, particularly low energies correspond to post-insertion intermediates presenting a *syn*-allyl coordination of the growing chain (Figure 4C,F).

The insertion pathways calculated for the three considered mechanisms are sketched as energy profiles for catalysts **1** and **5**, in parts A and B of Figure 5, respectively. For the sake of clarity, the monomer free

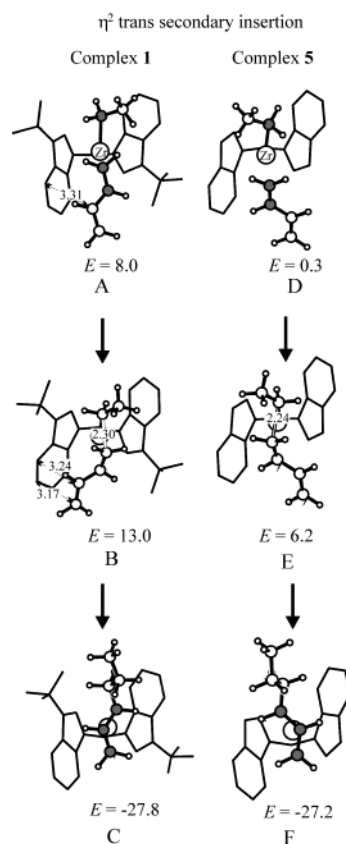


Figure 4. Models corresponding to mechanism i, which involves a η^2 s-trans secondary coordination of butadiene directly leading to a syn- η^3 -coordinated growing chain (Step D \rightarrow E of Scheme 1). Minimum energy monomer coordinated intermediates (A,D), transition states relative to the monomer insertion (B,E) and post-insertion intermediates (C,F), for catalysts **1** (A \rightarrow B \rightarrow C) and **5** (D \rightarrow E \rightarrow F).

species after an ethene monomer insertion, which is nearly identical for the three mechanisms, is also indicated in the sketches of Figure 5. Although the energy differences between these monomer free species and the corresponding monomer coordinated intermediates cannot be easily evaluated (mainly due to difficulty in defining the energy contribution associated with possible solvent and/or counterion coordination as well the entropy contribution), it is reasonable to assume that monomer coordination should lead to free energy increases of at least 5 kcal/mol.²²

The energy profiles of Figure 5A clearly show that, for catalyst **1**, which has bulky substituents in positions 3 and 3', mechanism i involving a η^2 primary butadiene insertion is largely favored. In fact, its activation energy relative to butadiene insertion is at least 4.5 kcal/mol smaller than for the other two competing mechanisms. This is in good agreement with the polymerization results of Table 1 and Table 2, since catalyst **1** for all the considered polymerization conditions, do not produce the usual 1,4- or 1,2-butadiene constitutional units but produces only constitutional units generated by the common intermediate, which presents a σ -coordinated backbiting growing chain (see Figure 2C and model B in Scheme 2).

On the other hand, the energy profiles of Figure 5B clearly show that, for the unsubstituted catalyst **5**, the activation energies of the three mechanism are nearly identical. This is in good agreement with the polymerization results of Table 1, showing that catalyst **5**, for

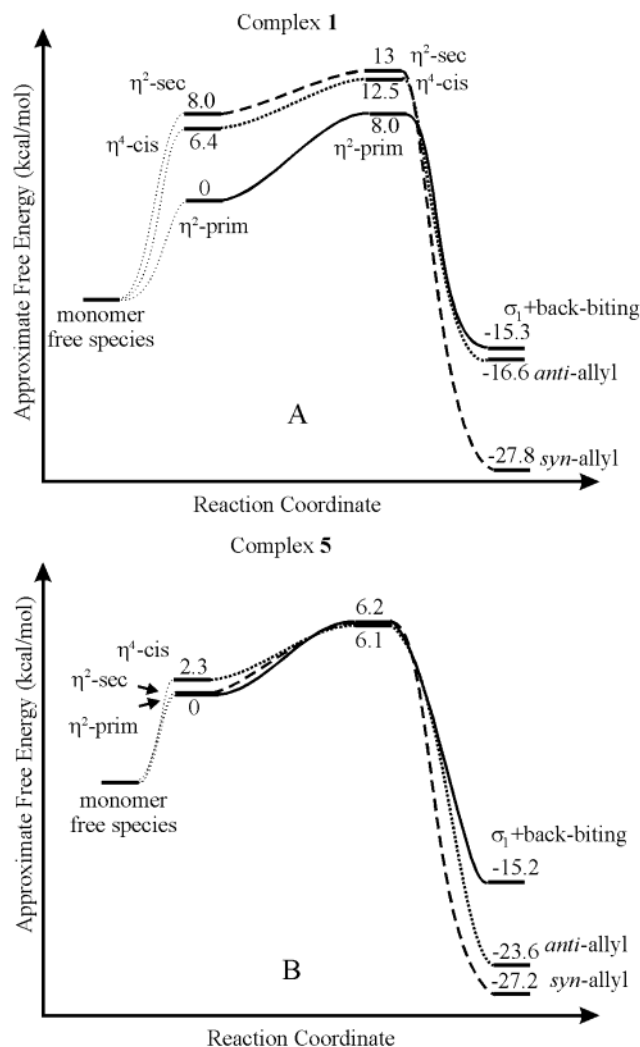


Figure 5. Energy profiles calculated for the three considered mechanisms, mainly based on the relative energies of models of Figures 2–4: (A) for catalysts **1**; (B) for catalyst **5**. The continuous lines correspond to the η^2 primary insertion of butadiene (mechanism i); the dotted lines correspond to the η^4 -s-cis insertion of butadiene (mechanism ii); the dashed lines correspond to the η^2 secondary insertion of butadiene (mechanism iii).

all the considered polymerization conditions, produce similar amounts of 1,4-*trans* units and of methylene-1,2-cyclopentane units. In the framework of the proposed mechanism, 1,4 *trans* units could be obtained directly from the *syn*-allyl intermediate of mechanism iii (Figure 4F) as well as after *anti* \rightarrow *syn* isomerization of the *anti*-allyl intermediate of mechanism ii (Figure 3F) while methylene-1,2-cyclopentane units would be generated by the intermediate which presents a σ -coordinated backbiting growing chain (Figure 2F; B \rightarrow C \rightarrow E route in Scheme 2).

The insertion transition state energy differences calculated for the three considered pathways are progressively reduced by decreasing the bulkiness of the substituent in position 3. However for metallocene **4**, where the substituent is simply a methyl group, the energy differences in favor of mechanism i are still 1.2 and 4.8 kcal/mol relative to mechanisms ii and iii, respectively. Also these molecular modeling results are in good agreement with the polymerization data of Table 1, since catalysts **2–4** for all the considered polymerization conditions produce essentially only con-

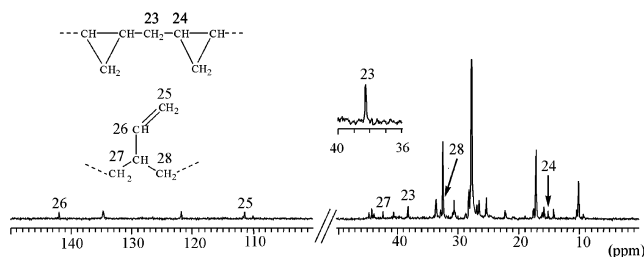


Figure 6. ^{13}C NMR spectrum of a samples **11** (hexamethyl-disiloxane scale). The inset models corespond to the additional substructures with respect to those of Figure 1. The inset spectral enlargement shows the narrow resonance of the methylene carbon located between two cyclopropane rings.

stitutional units generated by the intermediate which presents a σ -coordinated backbiting growing chain (B in Scheme 2).

It is worth noting that the minimum energy coordination intermediate and insertion transition state of Figure 2, parts A and B, present geometries very similar to those well established for isospecific propene insertion.^{12b,23} In fact, the chirality of the C_2 -symmetric metallocene imposes a *chiral orientation of the growing chain* (far from the bulky *tert*-butyl substituent) which in turn discriminates between the two possible enantiofaces of the coordinated butadiene. For instance, for the catalytic complexes of (*S,S*) chirality of Figure 2, at each insertion step, the butadiene insertion with the *si* enantioface is favored of nearly 4 kcal/mol, with respect to the insertion with the *re* enantioface. As a consequence, as already observed for cyclopolymerization reactions of nonconjugated α - ω dienes in the presence of isospecific C_2 -symmetric metallocenes,²⁴ beside the stereoselectivity of the cyclization reaction (leading to *trans*-1,2-cyclopropane and 1,2-cyclopentane units, as described in detail by the models of Figure 2 of ref 5) also a high stereoselectivity of the insertion reaction, leading to *trans*-diisotactic enchainment of the cyclic units, is expected.

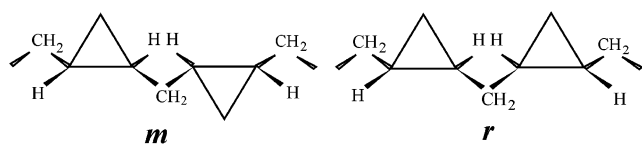
The above considerations relative to the stereoselectivity of butadiene primary insertion do not apply for catalysts **2–4**, whose isospecificity for propene polymerization is quite low.^{25,26}

Stereoselectivity of Butadiene Insertion by Catalyst 1. The model predictions of the previous section, relative to the stereoselectivity of butadiene insertion for catalyst **1**, can be verified by microstructural analysis of copolymers with large molar fraction of butadiene.

Just as an example, the copolymerization run 14 performed at 20 °C for 18 h, in the presence of catalytic precursors **1**, by using $[\text{B}] = 0.388$ mol/L, $[\text{E}]/[\text{B}] = 0.0016$, gave a yield of 0.150 g of a copolymer with a butadiene molar fraction $X_{\text{B}} = 0.12$. The ^{13}C NMR spectrum of this sample is reported in Figure 6, together with the additional recognized substructures corresponding to 1,2 inserted units of butadiene as well as two adjacent *trans*-methylene-1,2-cyclopropane units.

The 1,2-butadiene units can be recognized, respectively, by observing the signals at 111.4 and 142.0 ppm relative to methylene and methine of vinyl groups, as well as the signals at 42.6 and 32.4 ppm relative to the saturated adjacent methine and methylene. In these copolymerizations, at least at high concentration of butadiene, a relevant amount of 1,2-inserted units can be produced, since the coordination of butadiene is η^2 -primary.

Scheme 3



The two adjacent cyclopropane units can be recognized by observing the signals at 15.1 and 38.2 ppm relative to adjacent methine and methylene groups (carbons 24 and 23 of Figure 6, respectively). It is worth noting that the ^{13}C NMR signals relative to two adjacent *trans*-methylene-1,2-cyclopropane units are extremely narrow. This is more clearly shown by the inset enlargements of the methylene signal in Figure 6.

These data clearly indicate the presence of a high stereoregularity in the sequence of adjacent methylene-1,2-cyclopropane units, which is compatible with the large fraction of *m* dyads of *trans* 1,2-cyclopropane units, as suggested by the previous modeling section (see Scheme 3).

Conclusions

Copolymerization tests of 1,3-butadiene and ethene with catalytic systems based on C_2 -symmetric *ansa*-zirconocenes indicate that *trans*-1,4 constitutional units from butadiene are obtained essentially only for the metallocene **5**, which includes an unsubstituted bis(indenyl) ligand. The methylene-1,2-cyclopentane constitutional units from butadiene, which are obtained as a large fraction in the presence of metallocene **5**, can be obtained with high selectivity for metallocenes **4–3**, which include, in the C_2 symmetry related positions 3 and 3', methyl and ethyl substituents, respectively. The methylene-1,2-cyclopentane units can also be the main product also for copolymerizations in the presence of metallocene **2**, which includes in positions 3 and 3' isopropyl substituents, however substantial fractions of 1,1 and 1,3 as well of methylene-1,2-cyclopropane units are obtained. The methylene-1,2-cyclopropane units, become the main product for metallocene **1**, which includes in positions 3 and 3' bulky *tert*-butyl substituents. This is possibly related to the increasing difficulty, with increasing the bulkiness of the substituent in positions 3 and 3', of the cyclocopolymerization step leading to the cyclopentane rings ($B \rightarrow C$ in Scheme 2). For a complete understanding of this behavior, additional molecular modeling studies, aimed to a comparison of the two competing pathways leading to methylene-1,2-cyclopentane and to methylene-1,2-cyclopropane units (in Scheme 2, $B \rightarrow C \rightarrow E$ and $B \rightarrow D \rightarrow F$, respectively), have been planned.

The ratio between methylene-1,2-cyclopropane and methylene-1,2-cyclopentane units is poorly dependent on the polymerization conditions not only for metallocene **1**^{5,6} but also for metallocene **2**.

It is also worth noting that, as already described for catalyst **1**,⁶ also for metallocenes **2** and **3**, high polymerization temperatures and very low ethene concentrations in the feed can lead to formation of prevailing fractions of 1,1 and 1,3 constitutional units from butadiene.

Comparisons of the relative amount of constitutional units from butadiene obtained from polymerization tests conducted at different ethene concentrations indicate that, in the framework of the reactions of Scheme 2, the rate-determining step can be different for the different catalysts.

Molecular modeling calculations contribute to rationalize the observed behavior for copolymerizations of 1,3-butadiene with ethene catalyzed by these C_2 -symmetric metallocenes. For all the considered metallocenes, minimum energy coordination intermediates and insertion transition states have been located for the primary η^2 coordination of butadiene, which leads through a primary vinyl insertion to a σ -coordinated growing chain (step $A \rightarrow B$, in Scheme 2). The energy difference with respect to alternative butadiene coordination and insertion pathways are large not only for the bulkiest metallocene **1** but also for the other alkyl substituted metallocenes **2–4**. Only for the case of the unsubstituted metallocene **5**, the intermediate involving a primary η^2 coordination of butadiene and the corresponding insertion transition state leading to a σ -coordinated growing chain are nearly isoenergetic with the intermediate corresponding to the classical η^4 -*s-cis* coordination of butadiene and with the corresponding insertion transition state leading to a *anti*- η^3 -coordinated growing chain (step $A \rightarrow B$, in Scheme 1). Moreover, the molecular modeling calculations have shown that an additional nearly isoenergetic pathway can operate for butadiene coordination and insertion in ethene copolymerizations catalyzed by the unsubstituted metallocene **5**. This additional mechanism involves an η^2 *s-trans* secondary coordination of butadiene directly leading, after insertion, to a *syn*- η^3 -coordinated growing chain ($D \rightarrow E \rightarrow F$ in Scheme 1 and Figure 4D,E,F), which is the typical precursor of the *trans*-1,4 constitutional units from butadiene.

Molecular modeling also shows a high stereoselectivity for primary butadiene insertion on catalyst **1** (Figure 2 $A \rightarrow B \rightarrow C$), which is in agreement with the high stereoregularity which has been observed for adjacent methylene-1,2-cyclopropane units.

The new polymerization tests and molecular modeling results confirm the previous suggestion that all the unusual constitutional units from butadiene which are obtained for ethene copolymerizations catalyzed by metallocenes (methylene-1,2-cyclopentane, methylene-1,2-cyclopropane, and 1,3 and 1,1) are obtained as a consequence of different rearrangements of the σ -coordinated growing chain obtained after a butadiene primary vinyl insertion. On the other hand the *trans*-1,4 constitutional units from butadiene, which are obtained in substantial amounts only for the less hindered unsubstituted metallocene **5**, would be obtained by butadiene insertions leading to a growing chain allyl terminated and η^3 -coordinated to the metal.

Analogous molecular modeling calculations will be extended in the near future to the study of the homopolymerization of dienes with catalyst **1**, in the attempt to contribute to rationalize the unusual stereospecific behaviors which have been recently described.²⁷

Acknowledgment. The authors wish to thank Prof. L. Oliva and L. Cavallo for useful discussion and Dr. P. Oliva for technical assistance. Financial support from the "Ministero dell'Università e della Ricerca Scientifica e Tecnologica" (PRIN 2002, FISR Modelistica Molecolare project and Cluster C26 projects) is gratefully acknowledged.

Supporting Information Available: A table containing ^{13}C NMR chemical shifts of all structures reported in Figures 1 and 6 and tables of Cartesian coordinates of all modeled

structures. This material is available free of charge via the Internet at <http://pubs.acs.org>.

References and Notes

- (1) Welborn, H. C., Jr. Eur. Pat. EP0275676, 1988; *Chem. Abstr.* **1988**, 109, 150259z.
- (2) Galimberti, M.; Albizzati, E.; Abis, L.; Bacchilega, G. *Makromol. Chem.* **1991**, 192, 2591.
- (3) Morizono, K.; Okada, K.; Yamaguchi, M. U. S. Pat. 6,310,164, 2001.
- (4) Resconi, L.; Piemontesi, F.; Camurati, I.; Sundmeijer, O.; Ninfant'ev, I. E.; Ivchenko, P. V.; Kuz'mina, L. G. *J. Am. Chem. Soc.* **1998**, 120, 2308.
- (5) Pragliola, S.; Milano, G.; Guerra, G.; Longo, P. *J. Am. Chem. Soc.* **2002**, 124, 3502.
- (6) Longo, P.; Pragliola, S.; Milano, G.; Guerra, G. *J. Am. Chem. Soc.* **2003**, 125, 4799.
- (7) (a) Porri, L.; Giarrusso, A. In *Comprehensive Polymer Science*; Eastmond, G. C., Ledwith, A., Russo, S., Sigwalt, P., Eds.; Pergamon Press: Oxford, U.K., 1989; Vol. 4, Part II, p 53. (b) Taube, R.; Windisch, H.; Maiwald, S. *Macromol. Symp.* **1995**, 89, 393. (c) Guerra, G.; Cavallo, L.; Corradini, P.; Fusco, R. *Macromolecules* **1997**, 30, 677. (d) Costabile, C.; Milano, G.; Cavallo, L.; Guerra, G. *Macromolecules* **2001**, 34, 7952.
- (8) (a) Taube, R.; Gehrke, J.-P.; Radeaglia, R. *Organomet. Chem.* **1985**, 291, 101. (b) Tobish, S.; Taube, R. *Organometallics* **1999**, 18, 3045.
- (9) (a) Ewen, J. A. *J. Am. Chem. Soc.* **1984**, 106, 6355. (b) Longo, P.; Grassi, A.; Pellicchia, C.; Zambelli, A. *Macromolecules* **1987**, 20, 1015.
- (10) (a) Ewen, J. A.; Jones, R. L.; Razavi, A.; Ferrara, J. D. *J. Am. Chem. Soc.* **1988**, 110, 6255. (b) Guerra, G.; Longo, P.; Cavallo, L.; Corradini, P.; Resconi, L. *J. Am. Chem. Soc.* **1997**, 119, 4394.
- (11) (a) Grassi, A.; Zambelli, A.; Resconi, L.; Albizzati, E.; Maz-zocchi, R. *Macromolecules* **1988**, 21, 617.
- (12) (a) Röhl, W.; Brintzinger, H. H.; Rieger, B.; Zolk, R. *Angew. Chem., Int. Ed. Engl.* **1990**, 29, 339. (b) Toto, M.; Cavallo, L.; Corradini, P.; Moscardi, G.; Resconi, L.; Guerra, G. *Macromolecules* **1998**, 31, 3431.
- (13) Choo, T. N.; Waymouth, R. M. *J. Am. Chem. Soc.* **2003**, 125, 8970.
- (14) Caporaso, L.; Izzo, L.; Sisti, I.; Oliva, L. *Macromolecules* **2002**, 35, 4886.
- (15) ADF 2.3.0. Vrije Universiteit Amsterdam, Amsterdam, The Netherlands, 1996.
- (16) Baerends, E. J.; Ellis, D. E.; Ros, P. *Chem. Phys.* **1973**, 2, 41.
- (17) te Velde, B.; Baerends, E. J. *J. Comput. Phys.* **1992**, 99, 84.
- (18) Vosko, S. H.; Wilk, L.; Nusair, M. *Can. J. Phys.* **1980**, 58, 1200.
- (19) Becke, A. *Phys. Rev. A* **1988**, 38, 3098.
- (20) Perdew, J. P. *Phys. Rev. B* **1986**, 33, 8822.
- (21) Perdew, J. P. *Phys. Rev. B* **1986**, 34, 7406.
- (22) Chan, M. S. W.; Vanka, K.; Pye, C. C.; Ziegler, T. *Organometallics* **1999**, 18, 4624.
- (23) Corradini, P.; Cavallo, L.; Guerra, G. In *Metallocene-based Polyolefins*; Scheirs, J., Kaminsky, W., Eds.; Wiley: New York, 2000; Vol. 2, pp 1–36.
- (24) (a) Resconi, L.; Waymouth, R. M. *J. Am. Chem. Soc.* **1990**, 112, 4953. (b) Coates, G. W.; Waymouth, R. M. *J. Am. Chem. Soc.* **1991**, 113, 6270. (c) Kesti, M. R.; Waymouth, R. M. *J. Am. Chem. Soc.* **1992**, 114, 3565. (d) Coates, G. W.; Waymouth, R. M. *J. Mol. Catal.* **1992**, 76, 189. (e) Coates, G. W.; Waymouth, R. M. *J. Am. Chem. Soc.* **1993**, 115, 91. (f) Cavallo, L.; Guerra, G.; Corradini, P.; Resconi, L.; Waymouth, R. M. *Macromolecules* **1993**, 26, 260. (g) Ruiz de Ballesteros, O.; Venditto, V.; Auriemma, F.; Guerra, G.; Resconi, L.; Waymouth, R. M.; Mogstad, A. *Macromolecules*, **1995**, 28, 2383.
- (25) Cavallo, L.; Corradini, P.; Guerra, G.; Vacatello, M. *Polymer* **1991**, 32, 1329.
- (26) Ewen, J. A.; Elder, M. J.; Jones, R. L.; Haspeslagh, L.; Atwood, J. L.; Bott, S. G.; Robinson, K. *Makromol. Chem. Symp.* **1991**, 48/49, 253.
- (27) Pragliola, S.; Forlenza, E.; Longo, P. *Macromol. Rapid Commun.* **2001**, 22, 783.

MA034830J